Applied and Environmental Microbiology, July 2007, p. 4100–4109 Vol. 73, No. 13
0099-2240/07/$08.00+0 doi:10.1128/AEM.00360-07

Enterohemorrhagic *Escherichia coli* Biofilms Are Inhibited by 7-Hydroxyindole and Stimulated by Isatin▽†

Jintae Lee,[1] Tarun Bansal,[1] Arul Jayaraman,[1] William E. Bentley,[4] and Thomas K. Wood[1,2,3]*

Artie McFerrin Department of Chemical Engineering,[1] Department of Biology,[2] and Zachry Department of Civil Engineering,[3] 220 Jack E. Brown Building, Texas A&M University, College Station, Texas 77843-3122, and Fischell Department of Bioengineering, University of Maryland, College Park, Maryland 20742[4]

Received 13 February 2007/Accepted 26 April 2007

Since indole is present at up to 500 μM in the stationary phase and is an interspecies biofilm signal (J. Lee, A. Jayaraman, and T. K. Wood, BMC Microbiol. 7:42, 2007), we investigated hydroxyindoles as biofilm signals and found them also to be nontoxic interspecies biofilm signals for enterohemorrhagic *Escherichia coli* O157:H7 (EHEC), *E. coli* K-12, and *Pseudomonas aeruginosa*. The genetic basis of EHEC biofilm formation was also explored, and notably, virulence genes in biofilm cells were repressed compared to those in planktonic cells. In Luria-Bertani medium (LB) on polystyrene with quiescent conditions, 7-hydroxyindole decreased EHEC biofilm formation 27-fold and decreased K-12 biofilm formation 8-fold without affecting the growth of planktonic cells. 5-Hydroxyindole also decreased biofilm formation 11-fold for EHEC and 6-fold for K-12. In contrast, isatin (indole-2,3-dione) increased biofilm formation fourfold for EHEC, while it had no effect for K-12. When continuous-flow chambers were used, confocal microscopy revealed that EHEC biofilm formation was reduced 6-fold by indole and 10-fold by 7-hydroxyindole in LB. Whole-transcriptome analysis revealed that isatin represses indole synthesis by repressing *tnaABC* 7- to 37-fold in EHEC, and extracellular indole levels were found to be 20-fold lower. Furthermore, isatin repressed the AI-2 transporters *lsrABCDFGKR*, while significantly inducing the flagellar genes *flgABCDEFGHIJK* and *fliAEFGILMNOPQ* (which led to a 50% increase in motility). 7-Hydroxyindole induces the biofilm inhibitor/stress regulator *ycfR* and represses *cysADIJPU*/*fliC* (which led to a 50% reduction in motility) and *purBCDEFHKLMNRT*. Isogenic mutants showed that 7-hydroxyindole inhibits *E. coli* biofilm through cysteine metabolism. 7-Hydroxyindole (500 μM) also stimulates *P. aeruginosa* PAO1 biofilm formation twofold; therefore, hydroxyindoles are interspecies bacterial signals, and 7-hydroxyindole is a potent EHEC biofilm inhibitor.

Procaryotes and eucaryotes signal not only themselves but also one another; hence, there is competition and interference of cell signals. For example, interference of acylhomoserine lactones (AHLs) is manifested by AHL lactonases and acylases, which are present in both gram-positive and gram-negative bacteria (79). Similarly, autoinducer-2 (AI-2), a furanosyl borate diester or derivative (39), may be manipulated by *Escherichia coli* and *Vibrio harveyi* to interfere with the ability of each species to assess changes in cell population (75). This competition extends beyond procaryotes, as eucaryotes manipulate the quorum-sensing signals of bacteria, too. For example, algae block bacterial biofilm formation via furanones by controlling both AHL signaling (25) and AI-2 signaling (52), and mammals (including humans) block AHL signaling via lactonase in sera (76). Analogously, bacteria take advantage of eucaryotic signals since enterohemorrhagic *E. coli* O157:H7 (EHEC) bacteria utilize the human hormones epinephrine and norepinephrine to activate virulence genes (33), and bacteria interfere with plant indole 3-acetic acid-based signaling by using this signal as a source of carbon, nitrogen, and energy (37). Further evidence of this intense competition is that *E. coli* senses signals (AHLs) that it cannot synthesize to control biofilm formation (36a).

Other examples that confirm the importance of cell signaling for bacterial biofilm formation include the control of exopolysaccharide synthesis by quorum-sensing signals in *Vibrio cholerae* (22). In addition, AHLs control biofilm formation in *Pseudomonas aeruginosa* (10) and *Serratia liquefaciens* (36), and we have found that in vitro-synthesized AI-2 directly stimulates *E. coli* biofilm formation (20, 26). AI-2 has also been shown to control mutualistic biofilm formation (41, 55).

Extracellular indole is found at high concentrations (over 600 μM) when *E. coli* is grown in rich medium (12, 71) and was identified initially as a stationary-phase signal that controls *cysK*, *astD*, *tnaB*, and *gabT* (3) as well as *tnaAL* and *phoABU* (53). Recently, indole signaling has been shown to link plasmid multimerization and cell division (9), and indole was found to be a nontoxic interspecies signal that decreases biofilm formation in *E. coli* and increases the biofilms of *P. aeruginosa* and *P. fluorescens* (even though these pseudomonads do not produce this signal) (36a). We found that, in a manner analogous to that in which AHL signals bind SdiA (43, 78) and control biofilm formation in *E. coli* (36a), indole controls biofilms by inducing the AHL sensor of *E. coli*, SdiA, which influences cell motility and acid resistance (36a), even though *E. coli* does not produce AHL signals (43). Beyond biofilms, indole has been shown to control multidrug exporters (e.g., *acrDE* and *cusB*) in *E. coli* K-12 (28), to regulate the pathogenicity island of en-

* Corresponding author. Mailing address: 220 Jack E. Brown Building, Texas A&M University, College Station, TX 77843-3122. Phone: (979) 862-1588. Fax: (979) 865-6446. E-mail: Thomas.Wood@chemail.tamu.edu.

† Supplemental material for this article may be found at http://aem.asm.org/.

▽ Published ahead of print on 4 May 2007.

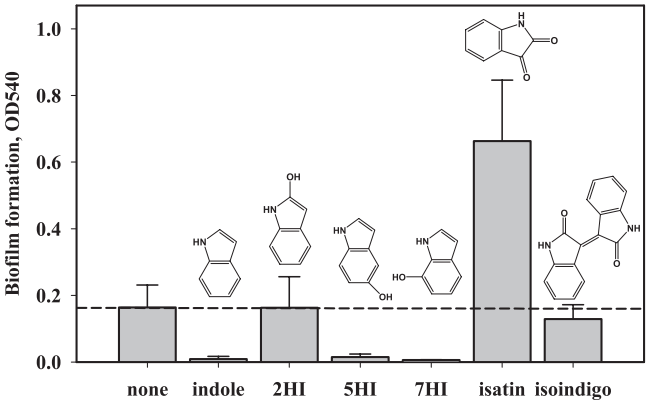

FIG. 1. Biofilm formation of EHEC in LB at 30°C after 7 h in 96-well plates with indole and hydroxyindoles. Indole, 2-hydroxyindole (2HI), 5-hydroxyindole (5HI), and 7-hydroxyindole (7HI) were used at 1,000 μM, whereas isatin and isoindigo were used at 250 μM. Each experiment was repeated two to four times with six wells each, and 1 standard deviation is shown. The structures of indole, 2HI, 5HI, 7HI, isatin, and isoindigo are shown.

teropathogenic *E. coli* (EPEC) (1), and to repress *gadX* of *E. coli* K-12 (36a), which activates virulence in EHEC (44).

Here, we focus on EHEC since it colonizes the large intestine, where its Shiga toxins cause hemorrhagic colitis and hemolytic-uremic syndrome (61). There are over 73,000 EHEC infections annually in the United States, which leads to 2,000 hospitalizations and 60 deaths, the economic cost of which is $405 million (18). It has been reported that EHEC forms biofilm on various surfaces (57, 69), and sloughing of the biofilm may cause contamination (57); however, an effective means of preventing EHEC biofilm formation has not been elucidated, and there is no effective treatment for EHEC infections, since antibiotic treatment increases the risk of hemolytic-uremic syndrome and renal failure (68, 73). We also tested the effect of hydroxylindoles on *P. aeruginosa* PAO1 since this strain is an opportunistic human pathogen (25).

Based on this proven competition for cell signals and given that indole controls biofilms (36a) and is present at up to 700 μM (12), we hypothesized that hydroxylated indoles (Fig. 1) may play a role in biofilm formation since many bacterial oxygenases, such as *Pseudomonas putida* PpG7 (15), *Ralstonia pickettii* PKO1 (16), *Pseudomonas mendocina* KR1 (67), and *Burkholderia cepacia* G4 (56), readily convert indole to oxidized compounds, such as 2-hydroxyindole, 3-hydroxyindole, 4-hydroxyindole, isatin, indigo, isoindigo, and indirubin (56). Using crystal violet staining and a continuous-flow chamber to study biofilm formation along with DNA microarrays to investigate the global transcriptome response, we show here that hydroxyindoles and isatin are interspecies biofilm signals that affect EHEC, *E. coli* K-12, and *P. aeruginosa* PAO1 by controlling biofilm-related genes, including those for AI-2 transport, indole synthesis, flagellar synthesis, and cysteine regulation. The genetic basis of EHEC biofilm formation was also investigated so that the impact of hydroxyindole signals on biofilm genes could be better interpreted.

MATERIALS AND METHODS

Bacterial strains, materials, and growth rate measurements. The strains and plasmids used are listed in Table 1. The EHEC strain used in this study was obtained from the American Type Culture Collection (ATCC 43895) and was a Centers for Disease Control isolate (EDL933) that was implicated in two outbreaks of hemorrhagic colitis in the United States during 1982; this strain produces Shiga toxins 1 and 2 (64). The *P. aeruginosa* PAO1 strain used in this study was the sequenced Holloway strain (63). LB (58) was used for all the experiments except for the motility assay. Indole, 4-hydroxyindole, 5-hydroxyindole, 7-hydroxyindole, isatin, indigo, and indirubin were purchased from Fisher Scientific (Pittsburgh, PA). 2-Hydroxyindole (oxindole) was purchased from Sigma Chemical (St. Louis, MO), and 6-hydroxyindole was obtained from Matrix Scientific (Columbia, SC). Isoindigo was prepared as described by Hoessel et al. (29, 56). To determine the toxicities of hydroxyindoles, the specific growth rates of EHEC planktonic cells were measured in LB medium at 37°C in the presence of hydroxyindoles (0, 250, 500, 1,000, and 2,000 μM), with dimethylformamide (DMF) added at 0.1 vol% to all samples; the experiments were performed twice using independent cultures. Purified AI-2 was synthesized as described previously (20).

Crystal violet biofilm assay. The crystal violet biofilm assay was adapted (49); overnight cultures were diluted to a turbidity of 0.05 at 600 nm and were incubated in polystyrene 96-well plates at 30°C for 7 h or 24 h without shaking in LB medium. Each data point was averaged from at least 12 replicate wells (6 wells from two independent cultures). The experiments were performed two or four times using independent cultures.

Flow chamber biofilm experiments. The inoculum and biofilm growth medium was LB supplemented with 300 μg/ml erythromycin to maintain pCM18 (24) and thus to retain the constitutive green fluorescent protein (GFP) vector for visualizing the biofilm. The biofilm was formed at 30°C in a continuous-flow chamber that consisted of a standard glass microscope slide on one side and a plastic coverslip on the other side, with dimensions of 47.5 mm by 12.7 mm and a 1.6-mm gap between the surfaces (BST model FC81; Biosurface Technologies Corp., Bozeman, MT), and was visualized with confocal microscopy as described

TABLE 1. Strains and plasmids used in this study[a]

Strain or plasmid	Description or genotype	Reference
Strains		
E. coli O157:H7	EHEC Stx1$^+$ and Stx2$^+$	64[b]
E. coli K-12 BW25113	*lacI*^{q} *rrnB*$_{T14}$ Δ*lacZ*$_{WJ16}$ *hsdR514* Δ*araBAD*$_{AH33}$ Δ*rhaBAD*$_{LD78}$	2
E. coli K-12 BW25113 Δ*cysB*	K-12 BW25113 Δ*cysB* Ω Km^r	2
P. aeruginosa PAO1	Wild type	63
Vibrio harveyi BB170	BB120 *luxN*::Tn*5* (AHL sensor negative, AI-2 sensor positive)	66
E. coli UT481/pCX39	Δ*lac-pro met pro zzz*::Tn*10 thy supD* r_K^- m_K^- *ftsQ2p*::*lacZ* Amp^r	19
Plasmids		
pCM18	Em^r; pTRKL2-P$_{CP25}$-RBSII-*gfp*mut3*-T$_0$-T$_1$ (GFP plasmid for visualizing biofilm)	24
pCA24N-*cysB*$^+$	Cm^r; *lacI*^{q} pCA24N P$_{T5\text{-}lac}$::*cysB*$^+$	35

[a] Km^r, Amp^r, Em^r, and Cm^r are the antibiotic resistance phenotypes for kanamycin, ampicillin, erythromycin, and chloramphenicol, respectively, and Stx is the Shiga toxin.
[b] ATCC 43895.

previously (74). The inocula were diluted to a turbidity of 0.2 at 600 nm and used to seed the flow cell for 2 h at 10 ml/h before fresh LB erythromycin medium was added at the same flow rate. To study the effect of indole and 7-hydroxyindole on biofilm formation, the compounds were dissolved in DMF and added at 1,000 μM in the continuous feed upon inoculation; DMF was added as the negative control to the no-hydroxyindole flow chamber. The initial inoculum was 1.9×10^8 to 4.7×10^8 cells/ml. Each flow chamber experiment was repeated two times (six experiments). A dispersion experiment was also performed with 7-hydroxyindole by adding 1,000 μM in the 10-ml/h feed after biofilm formation for 24 h in LB erythromycin medium in the absence of hydroxyindole. GFP allowed visualization of the EHEC biofilm by excitation with an Ar laser at 488 nm (emission, 500 to 600 nm), using a TCS SP5 scanning confocal laser microscope with a 63× HCX PL FLUOTAR L dry objective, a correction collar, and a numerical aperture of 0.7 (Leica Microsystems, Mannheim, Germany).

Color confocal flow cell images were converted to gray scale (74), and biomass, substratum coverage, surface roughness, and mean thickness were determined using COMSTAT image-processing software (27) as described previously (74). For each experiment, nine different random positions were chosen for microscope analysis, and 25 images were processed for each point. Values are means of data from the different positions at the same time point, and standard deviations were calculated based on these mean values for each position. Simulated three-dimensional images were obtained using IMARIS (BITplane, Zurich, Switzerland). Twenty-five pictures were processed for each three-dimensional image.

Motility assay. LB overnight cultures were used to assay motility in plates containing 1% tryptone, 0.25% NaCl, and 0.3% agar (62) by measuring halos at 20 h at 37°C. When the effect of isatin and 7-hydroxyindole on motility was tested, isatin (50 μM) and 7-hydroxyindole (1,000 μM) dissolved in DMF were added to the motility agar. DMF (0.1%) was added as the negative control. Each experiment was performed two times using two independent cultures, with each culture evaluated in triplicate.

Biofilm total RNA isolation for DNA microarrays. For the microarray experiments, 10 g glass wool (Corning Glass Works, Corning, NY) was used to form biofilms (51) in 250 ml of LB in 1-liter Erlenmeyer shake flasks which were inoculated with overnight cultures that were diluted 1:167. 7-Hydroxyindole (1,000 μM) in 250 μl DMF, isatin (250 μM) in 250 μl DMF, or 250 μl DMF alone was added. The cells were shaken at 250 rpm and 30°C for 7 h to form biofilms on the glass wool. The glass wool was removed from the culture quickly and gently washed two times in 100 ml 0.85% NaCl buffer at 0°C (less than 30 seconds). Biofilm cells were removed from glass wool by sonication for 2 min in 200 ml of 0.85% NaCl buffer at 0°C, and cell pellets were stored at −80°C until used. RNA was isolated from the planktonic and biofilm cells as described previously (51).

DNA microarrays. An *E. coli* GeneChip 2.0 genome array (product no. 900551; Affymetrix, Santa Clara, CA) was used to study the differential gene expression profile of the EHEC biofilm after addition of 7-hydroxyindole and isatin as described in the gene expression technical manual; the array contains 10,208 probe sets for open reading frames, rRNA, tRNA, and intergenic regions for four *E. coli* strains: MG1655, CFT073, O157:H7-Sakai, and O157:H7-EDL933 (EDL933 was used in this study). Hybridization was performed for 16 h, and the total cell intensity was scaled automatically in the software to an average value of 500. The data were inspected for quality and analyzed according to the procedures described in Data Analysis Fundamentals, which includes use of premixed polyadenylated transcripts of the *Bacillus subtilis* genes (*lys*, *phe*, *thr*, and *dap*) at different concentrations. Genes were identified as differentially expressed if the change in *P* value was less than 0.05 and the expression ratio was greater than threefold for biofilm versus planktonic cells, twofold for 7-hydroxyindole, or fourfold for isatin, since the standard deviations were 2.3 for biofilm versus planktonic cells, 1.5 for 7-hydroxyindole addition, and 3.9 for isatin addition. Gene functions were obtained from the Affymetrix-NetAffx analysis center.

Real-time PCR. To corroborate the DNA microarray data, the transcription levels of four genes were quantified using real-time reverse transcription-PCR (RT-PCR) (70). The same total RNA used for the Affymetrix microarrays was used for these studies. The primers were designed using PrimerQuest online software (Table 2). The real-time RT-PCR was performed using an iScript one-step RT-PCR kit with SYBR green (Bio-Rad Laboratories, CA) on a MyiQ single-color real-time PCR detection system (Bio-Rad Laboratories). The threshold cycles, as calculated by the MyiQ optical system software (Bio-Rad Laboratories), were used to determine the relative changes between the samples. The experiments were run in triplicate in 20 μl, and 50 ng of total RNA was used for each reaction, with the final forward and reverse primer concentrations at 0.5 μM each. After amplification, template specificity was ensured by using melting-curve analysis. *rrsG* was used as the housekeeping gene for normalizing the data.

TABLE 2. Primers used for RT-PCR

Gene	Forward primer	Reverse primer
lsrA	5′-AACATCCTGTTTGGGCTGGCAA-3′	5′-AAACAAGCGTTCGGTTTCCGCA-3′
lsrB	5′-AGCATCCTGGCTGGGAAATTGT-3′	5′-AAATTCTTTCACCGTGCCGCGT-3′
lsrC	5′-ACAGCGTTTGGACGCAGTTT-3′	5′-ACGCAGGCTGCAATTGCTTT-3′
cysP	5′-AACCCGCCGTTTGAACAGCAAT-3′	5′-TGGATATTCTTCGGGTTGCCCT-3′
rrsG	5′-TATTGCACAATGGGCGCAAG-3′	5′-ACTTAACAAACCGCCTGCGT-3′

AI-2, indole, and β-galactosidase assays. The activity of the synthesized AI-2 was assayed as described previously (66). Briefly, the reporter strain *V. harveyi* BB170 was grown in AB medium overnight and diluted 1:5,000 in fresh AB medium, and then supernatants from *E. coli* LB cultures with 250 μM isatin (harvested at 7 h) were added to the AI-2 reporter strain. Bioluminescence was measured with a 20/20 luminometer (Turner Design, Sunnyvale, CA) and reported as relative light units. The cell density of the *V. harveyi* reporter strain was measured by spreading the cells on LM plates and counting CFU after 24 h. The experiment was performed in duplicate.

Extracellular and intracellular indole concentrations from cells in LB medium were measured spectrophotometrically in duplicate as described previously (12), by modifying the protocol of Kawamura-Sato et al. (34). Also, the spectrophotometric indole assay was corroborated with reverse-phase high-performance liquid chromatography (HPLC) using a 100- by 4.6-mm Chromolith Performance RP-18e column (Merck KGaA, Darmstadt, Germany) and gradient elution, with H_2O-0.1% formic acid and acetonitrile as the mobile phases, at a flow rate of 1 ml/min (65:35 for 0 to 5 min, 35:65 for 5 to 12 min, and 65:35 at 12 min). Under these conditions, the retention times and the absorbance maxima were 3.6 min/264 nm for 7-hydroxyindole and 5.9 min/271 nm for indole.

E. coli UT481 harboring pCX39 (*ftsQ2p*::*lacZ*) (19) was grown at 30°C with 100 μg ampicillin/ml from diluted overnight cultures to a turbidity of 2 at 600 nm. The β-galactosidase activities were calculated based on a protein concentration of 0.31 mg protein/ml/OD_{600}. A modified Lowry protein assay kit from Pierce Biotechnology (Rockford, IL) was used to measure the total protein content.

7-Hydroxyindole degradation. For the degradation of 7-hydroxyindole, overnight EHEC cultures grown in LB were diluted to a turbidity at 600 nm of 0.05 and were regrown in LB with 1,000 μM 7-hydroxyindole for 24 h at 30°C at 250 rpm. As a negative control, autoclaved cells at a turbidity of 0.05 were contacted with 7-hydroxyindole under the same conditions to confirm that there was no evaporation or adsorption. To confirm the lack of hydroxyindole production from either indole or 7-hydroxyindole by EHEC, exponentially grown cells (OD_{600}, ~2.0) were harvested and resuspended in 50 mM Tris-HCl buffer (pH 7.4; OD_{600}, ~10.0) and were contacted with 1,000 μM indole or 7-hydroxyindole for 1 h. Each experiment was performed two times using two independent cultures.

Microarray data accession number. The expression data for the biofilm samples were deposited in the NCBI Gene Expression Omnibus and are accessible through accession number GSE6195 (4, 14).

RESULTS

The goals of this research were to determine if hydroxyindoles influence biofilm formation of EHEC, *E. coli* K-12, and *P. aeruginosa* PAO1 and then to explore the genetic basis of this control. The genetic basis for EHEC biofilm formation was also evaluated using DNA microarrays since this has not been previously investigated and this facilitates gauging the impact of hydroxyindoles on biofilm genes.

Toxicity. To test the toxicities of hydroxyindoles on EHEC, indole, 5-hydroxyindole, 7-hydroxyindole, and isatin were tested in LB at 37°C. In the absence of hydroxyindoles, the specific growth rate was 1.43 ± 0.09/h, whereas the growth rates were 1.38 ± 0.01/h with 1,000 μM indole, 1.48 ± 0.08/h

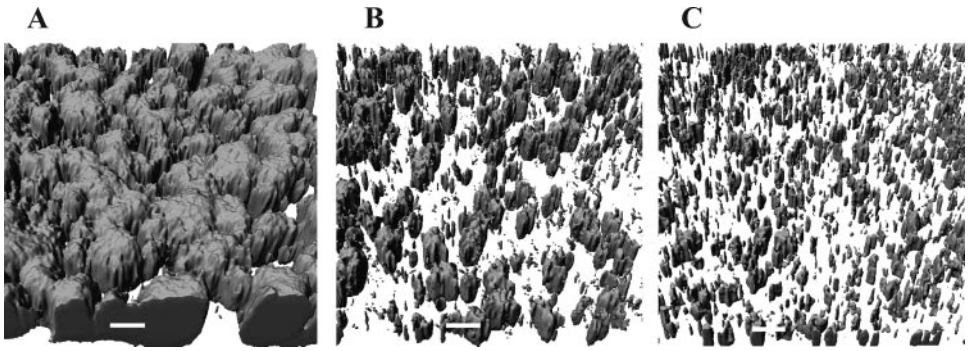

FIG. 2. EHEC biofilm formation in LB at 30°C after 24 h in flow cells without an indigoid compound but with the diluent DMF (A), with 1,000 μM indole (B), and with 1,000 μM 7-hydroxyindole (C). Each experiment was repeated two times, and one representative image is shown. The scale bar indicates 20 μm.

with 1,000 μM 5-hydroxyindole, 1.14 ± 0.03/h with 1,000 μM 7-hydroxyindole, and 1.44 ± 0.04/h with 250 μM isatin. Hence, these indigoids do not significantly change the specific growth rate of EHEC. For 5-hydroxyindole, concentrations as high as 2,000 μM did not affect cell growth (1.40 ± 0.05/h). In addition, indole, 5-hydroxyindole, 7-hydroxyindole, and isatin at 500 μM were not toxic to *P. aeruginosa* PAO1.

Hydroxyindoles inhibit and stimulate EHEC biofilm formation. In the absence of hydroxyindoles, it was observed that EHEC formed robust biofilms at 30°C and at 37°C after 24 h although those at 30°C were larger; hence, all the biofilm results here are reported at 30°C. Since indole (36a) and hydroxyindoles were not toxic to EHEC, we screened various hydroxyindoles (Fig. 1) for their abilities to inhibit EHEC in 96-well plates in LB for 9 h at 30°C (similar results were found at 37°C): 2-hydroxyindole, 4-hydroxyindole, 5-hydroxyindole, 6-hydroxyindole, 7-hydroxyindole, and isatin were screened at 500 μM, and indigo, isoindigo, and indirubin were screened at 250 μM since they were insoluble in water above 250 μM. We chose concentrations of 250 to 1,000 μM since EHEC produced 362 ± 3 μM indole after 8 h and K-12 produced 403 ± 8 μM, as found through two independent assays. Indole, 5-hydroxyindole, and 7-hydroxyindole were the most effective at reducing EHEC biofilm formation (more than 50%), 4-hydroxyindole decreased biofilm by about 50%, and isatin increased EHEC biofilm (data not shown). After the preliminary screening, 1,000 μM concentrations of indole, 2-hydroxyindole, 5-indroxyindole, and 7-hydroxyindole as well as 250 μM isatin and isoindigo were tested for their impacts on biofilm formation of EHEC in LB at 30°C for 7 h. Biofilm formation was clearly inhibited by indole (18-fold), 5-hydroxyindole (11-fold), and 7-hydroxyindole (27-fold), whereas biofilm formation was stimulated by isatin (4-fold) and was not affected by 2-hydroxyindole and isoindigo (Fig. 1). Furthermore, isatin from 0 to 1,000 μM stimulated biofilm formation in a dose-dependent manner, and 7-hydroxyindole from 0 to 2,000 μM inhibited biofilm formation in a dose-dependent manner (data not shown). Therefore, use of double hydroxylation of indole to form isatin increased biofilm formation whereas the position of the single hydroxyl group had a profound effect on the efficacies of these biofilm inhibitors.

The effects of 7-hydroxyindole, the most potent biofilm inhibitor out of the 9 tested hydroxyindoles, and indole were investigated using a more rigorous continuous-flow chamber with EHEC in LB medium at 30°C. As shown in Fig. 2A, EHEC forms robust biofilms with undulating towers interspersed with water channels in rich medium at 30°C at 24 h. To our knowledge, this is the first EHEC biofilm image in a continuous-flow chamber. Upon addition of indole at 1,000 μM, biofilm formation was reduced and consisted of individual slender microcolonies (Fig. 2B). Upon addition of 7-hydroxyindole at 1,000 μM, the microcolonies became significantly smaller, scattered towers (Fig. 2C). These visual results were quantified using COMSTAT, indicating that addition of indole reduced biofilm mass 6-fold (7.9 ± 3 versus 46 ± 6 $\mu m^3/\mu m^2$) and reduced mean biofilm thickness 4-fold (14 ± 5 versus 55 ± 5 μm), and addition of 7-hydroxyindole reduced biofilm mass 10-fold (4.5 ± 3 versus 46 ± 6 $\mu m^3/\mu m^2$) and reduced mean biofilm thickness 5.5-fold (10 ± 5 versus 55 ± 5 μm). Hence, 7-hydroxyindole was more effective than indole in decreasing EHEC biofilms. The results for the two independent experiments using the flow chamber for each application of DMF alone, indole, and 7-hydroxyindole were consistent.

To confirm the presence of hydroxyindoles, the extracellular indole and 7-hydroxyindole concentrations were measured in the effluent of the flow chamber by using HPLC. The level of indole without indole addition ranged from 1 to 8 μM at 24 h, while the level of indole was maintained above 185 μM for 24 h upon addition of indole (1,000 μM), and the level of 7-hydroxyindole was maintained above 540 μM for 24 h upon addition of 7-hydroxyindole (1,000 μM). Note that extracellular concentrations of indole are complex since EHEC both synthesizes and degrades indole via its reversible tryptophanase (TnaA) (47) and since it imports indole via Mtr (77). Also, it was found here that EHEC degrades 7-hydroxyindole at a rate of 0.60 ± 0.03 nmol/mg protein/min (from 1,100 μM to 380 μM for 24 h). Furthermore, added indole and 7-hydroxyindole were not converted into other hydroxyindoles in EHEC. Hence, the changes in EHEC biofilm formation are due to the presence of indole and 7-hydroxyindole.

To investigate whether 7-hydroxyindole disperses the existing strong biofilm, 7-hydroxyindole (1,000 μM) was added after biofilm formation for 24 h in LB. During the following 24 h, there was no new biofilm formed; however, no significant dispersion was observed (data not shown).

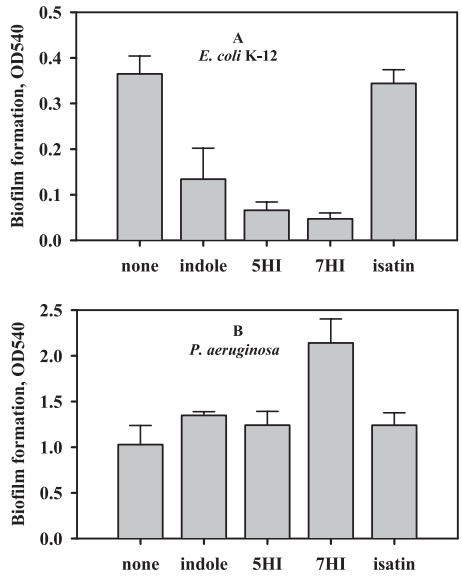

FIG. 3. Biofilm formation in LB at 30°C after 24 h in 96-well plates for *E. coli* K-12 BW25113 with 1,000 μM indole, 1,000 μM 5-hydroxyindole (5HI), 1,000 μM 7-hydroxyindole (7HI), and 250 μM isatin (A) and for *P. aeruginosa* PAO1 with 500 μM indole, 500 μM 5-hydroxyindole (5HI), 500 μM 7-hydroxyindole (7HI), and 250 μM isatin (B). Each experiment was repeated two to four times with six wells each, and 1 standard deviation is shown.

Hydroxyindoles inhibit *E. coli* K-12 biofilm and stimulate *P. aeruginosa* PAO1 biofilm. Along with the result for EHEC, the effect of hydroxyindoles on the biofilm formation of *E. coli* K-12 BW25113 was evaluated using the crystal violet assay. 5-Hydroxyindole and 7-hydroxyindole significantly inhibited *E. coli* K-12 biofilm formation, as with EHEC (Fig. 3A). However, isatin did not affect *E. coli* K-12 biofilm formation significantly (Fig. 3A), whereas isatin increased EHEC biofilm. Since *E. coli* K-12 produces high concentrations of extracellular indole when *E. coli* is grown in rich medium (over 600 μM) (12, 71), the levels of extracellular indole were measured from *E. coli* K-12 and EHEC shake flasks at 30°C for 24 h. *E. coli* K-12 produced 401 ± 11 μM indole, and EHEC produced 308 ± 12 μM indole at 24 h. The lower concentrations of extracellular indole for EHEC than for *E. coli* K-12 may partially explain the higher level of biofilm formation for EHEC than for *E. coli* K-12 (crystal violet density, 1.76 ± 0.15 versus 0.37 ± 0.04 at 30°C at 24 h).

To determine if hydroxyindoles are signals for pseudomonads too, we added indole, 5-hydroxyindole, 7-hydroxyindole, and isatin to *P. aeruginosa* PAO1. There was a significant increase in biofilm formation for *P. aeruginosa* PAO1 with 7-hydroxyindoles (Fig. 3B). Indole, 5-hydroxyindole, and isatin at 500 μM increased *P. aeruginosa* PAO1 biofilm formation by 20 to 30%, and 7-hydroxyindole (500 μM) increased biofilm formation twofold (Fig. 3B). It is notable that EHEC produces indole but *P. aeruginosa* alone does not produce indole or any hydroxyindoles in LB after 24 h and that indole and 7-hydroxyindole inhibit EHEC biofilm but enhance *P. aeruginosa* biofilm without cell growth inhibition. Also, it has been previously shown that *Pseudomonas* cells engineered to express toluene *o*-monooxygenase increase *E. coli* biofilm formation by decreasing indole concentration (36a). Therefore, we suggest that indole and hydroxyindoles are interspecies biofilm signals.

Differential gene expression in 7-h EHEC biofilms. To investigate the global genetic basis of hydroxyindole regulation of EHEC biofilm formation, DNA microarrays were first used to determine differential gene expression for EHEC biofilm cells versus planktonic cells. It was found that 402 genes were regulated significantly (more than threefold) in biofilms; 119 genes were induced, and 283 were repressed. Most noticeable was that in biofilm cells, 20 pathogenic genes of the locus of enterocyte effacement (LEE) operon (a total of 54 genes in EDL933) (48) were highly repressed (3- to 11-fold) (see Table S1 in the supplemental material). Also, 13 genes of the *wca* operon (*wcaABCDEFGHIJKL* and *rcsA*) that are involved in colanic acid synthesis and biofilm formation (50) and 6 fimbrial genes (*fimB*, *ycbQRS*, *ybgD*, and Z1538) were repressed in the biofilm cells (see Table S1 in the supplemental material). Nitrate reductase genes (*narGHIJK*) and the galactitol phosphotransferase (PTS) family of genes (*agaVWYZ*) that are involved in the synthesis of dihydroxyacetone phosphate (8) were both induced in the biofilm cells (see Table S1 in the supplemental material).

Since EHEC from an aggregative colony forms more biofilm than cells from a smooth colony (69), aggregation of EHEC and *E. coli* K-12 was also measured in LB at 30°C for 24 h. EHEC formed sevenfold more aggregates than *E. coli* K-12, which suggests that the highly aggregative behavior of EHEC may be related to its ability to form robust biofilms.

Differential gene expression with 7-hydroxyindole in 7-h EHEC biofilms. Since hydroxyindoles affected biofilm formation (Fig. 1 and 2), we focused on differential gene expression in the biofilm itself rather than on planktonic cells. 7-Hydroxyindole (1,000 μM) significantly regulated (more than twofold) 347 genes, with 93 genes induced and 254 genes repressed (see Table S1 in the supplemental material). Among the repressed genes, 12 genes related to purine nucleotide biosynthesis (*purBCDEFHKLMNRT*) were repressed 3- to 12-fold; previously, we found that AI-2 repressed the *purDEFHKMT* operon in K-12 (52). In addition, genes related to cysteine biosynthesis (*cysADIJPU*) were repressed 4- to 11-fold, and previously, we found that the nontoxic biofilm inhibitor ursolic acid repressed *cysDJK* (54). Carbamoyl phosphate synthetase genes (*carAB*) were also repressed (see Table S1 in the supplemental material).

Although indole inhibits *E. coli* K-12 biofilm formation through SdiA (36a), 7-hydroxyindole did not change *sdiA* expression (via microarrays) in EHEC biofilm. To investigate this further, transcription of the SdiA-controlled promoter *ftsQ2p* (19) was investigated using a β-galactosidase reporter; unlike indole (36a), neither 7-hydroxyindole nor isatin altered *ftsQ2p* expression significantly. Hence, these hydroxyindoles do not appear to work through SdiA.

Among the induced genes were ribonucleoside-diphosphate reductase operon genes (*nrdHIEF*), propionate metabolism genes (*prpCDE*), nitrate reductases (*narVZ*), the biofilm stress regulator *ycfR* (80), and a hypothetical gene (*yhcN*). Also repressed were hydrogen uptake genes (*hyaABCDEF*) and motility-related genes (*fliC*, c1936) (see Table S1 in the supplemental material).

To confirm the presence of 7-hydroxyindole, the extracellu-

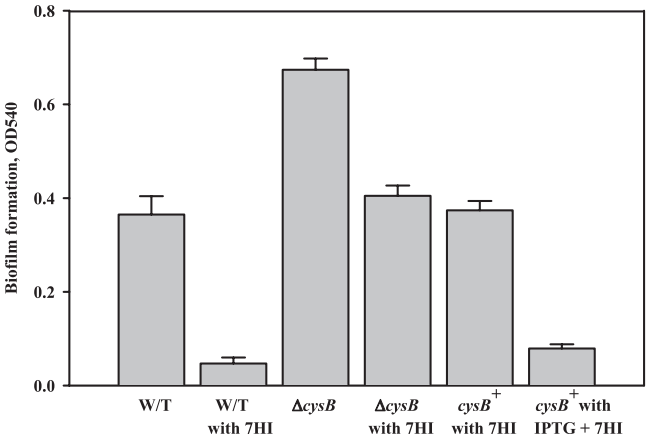

FIG. 4. Biofilm formation in LB at 30°C after 24 h in 96-well plates with expression of *cysB*$^+$ (via 1 mM IPTG) and addition of 7-hydroxyindole (7HI, 1,000 μM) with *E. coli* K-12 BW25113 Δ*cysB*/pCA24N-*cysB*$^+$. Each experiment was repeated two times with six wells each, and 1 standard deviation is shown. The wild type (WT) is BW25113, Δ*cysB* is BW25113 Δ*cysB*, and *cysB*$^+$ is BW25113 Δ*cysB*/pCA24N-*cysB*$^+$.

lar 7-hydroxyindole concentration was measured using HPLC when the biofilm cells were prepared for the microarray experiment. The level of 7-hydroxyindole was 550 μM in a shake flask at 7 h, which matches well with the extracellular 7-hydroxyindole (540 μM) concentration found in the flow chamber at 24 h.

Motility and 7-hydroxyindole. Since it has been reported that motility is essential for initial cell attachment in *E. coli* biofilm formation (49) and since the microarray data showed that several flagellar genes (c1936, *fliC*, and *motB*) were repressed by 7-hydroxyindole (see Table S1 in the supplemental material), the motility of EHEC was tested using a swimming assay (62). 7-Hydroxyindole decreased motility by 53% (2.3 ± 0.5 cm without hydroxyindole versus 1.1 ± 0.1 cm with 1,000 μM 7-hydroxyindole after 20 h). Therefore, the reduction in cell motility upon addition of 7-hydroxyindole may contribute to the inhibition of EHEC biofilm formation.

Cysteine metabolism and 7-hydroxyindole. Since 7-hydroxyindole repressed the cysteine synthesis operon *cysADEIJP* 4- to 11-fold (see Table S1 in the supplemental material), we tested the effect of overproducing CysB via pCA24N-*cysB*$^+$ in an *E. coli* K-12 *cysB* mutant while adding hydroxyindoles. CysB positively regulates the biosynthesis of cysteine in *E. coli* (46), and deletion of *cysB* increased biofilm formation (Fig. 4), as has been previously reported (54). Addition of 1,000 μM 7-hydroxyindole to the *cysB* mutant resulted in a 1.8-fold reduction of biofilm (Fig. 4), while addition of 1,000 μM 7-hydroxyindole to the K-12 wild type resulted in a 7.7-fold reduction of biofilm (Fig. 4); hence, 7-hydroxyindole is less effective in the absence of CysB. Also, induction of *cysB* (via addition of 1 mM IPTG (isopropyl-β-D-thiogalactopyranoside) to induce *cysB*$^+$ from pCA24N-*cysB*$^+$) in the presence of 1,000 μM 7-hydroxyindole resulted in a 4.7-fold greater reduction in biofilm (Fig. 4). Similar results were found with EHEC that overproduces CysB from pCA24N-*cysB*$^+$. Expression of *cysB* with 1 mM IPTG made 1,000 μM 7-hydroxyindole 10-fold ± 3-fold more effective in reducing biofilm formation (note that these experiments differ from those for Fig. 1, which lacked the *cysB*$^+$ plasmid and were conducted at 7 h). Hence, overproducing CysB dramatically improved the effectiveness of 7-hydroxyindole, which implies that this biofilm inhibitor works through the cysteine biosynthesis pathway.

Differential gene expression with isatin in 7-h EHEC biofilms. Isatin (250 μM) significantly regulated (more than fourfold) 552 genes, with 151 genes induced and 401 genes repressed (see Table S1 in the supplemental material). Among the repressed genes were eight genes related to the AI-2 transporters (*lsrABCDFGKR*), indole biosynthesis genes (*tnaABC* and *yliH*), cysteine desulferase genes (*sufABCDES*), nitrate reductase genes (*narHIJUVWYZ*), hydrogen uptake genes (*hyaABCDEF*), propionate metabolism genes (*prpBCDE*), and acid resistance-related genes (*gadABC*) (see Table S1 in the supplemental material).

The genes most significantly induced by isatin were flagellar genes (*flgABCDEFGHIJK* and *fliAEFGILMNOPQ*), 44 various transport genes (e.g., *proVWX* and *cirA*), and *treBC*, which encode the trehalose PTS permease and trehalose-6-phosphate hydrolase (6). Based on the induction of the flagellar genes, we investigated the effect of isatin addition (50 μM) on motility and found that it was increased by 47% ± 8%; therefore, the increase in cell motility upon addition of isatin may contribute to the stimulation of EHEC biofilm formation. Note that among the genes differentially expressed in response to isatin (increased biofilm) and 7-hydroxyindole (decreased biofilm), the motility-related genes (*fliC*, c1936, and *motAB*), nitrate reductase genes (*narUVWYZ*), propionate metabolism genes (*prpBCDE*), carbamoyl phosphate synthetase genes (*carAB*), transport genes (*yieG*, *lldP*, *uraA*, and *sdaC*) and *phoH*, *ompF*, and *fis* genes were oppositely regulated (see Table S1 in the supplemental material).

Isatin, indole, and AI-2. Based on the DNA microarray data with isatin, we investigated indole concentrations with 250 μM isatin since *tnaA* was repressed sevenfold with this compound (see Table S1 in the supplemental material). It was found that isatin represses extracellular indole concentrations 20-fold ± 13-fold in EHEC. Since extracellular indole represses biofilms (11, 12, 36a, 80), it appears that isatin increases EHEC biofilm formation by dramatically decreasing indole concentrations. It was also found that isatin reduced intracellular indole concentration 2.6-fold ± 0.5-fold, while 7-hydroxyindole had no effect on intracellular indole concentration.

Since the AI-2 transporter genes (*lsrABCDFGKR*) were highly regulated by the addition of isatin (see Table S1 in the supplemental material), we investigated the impact of purified AI-2 on EHEC biofilm formation. We found that 50 μM AI-2 increased EHEC bottom biofilm formation in LB medium 3.0-fold ± 0.7-fold after 15 h and 10-fold ± 2.5-fold after 24 h; total biofilm was increased 1.6-fold ± 0.2-fold after 24 h. Therefore, AI-2 increases EHEC liquid/solid biofilm formation as it does that of K-12 (20).

Verification of microarray results by RT-PCR. RT-PCR was used to verify gene expression for *lsrA*, *lsrB*, and *lsrC* for the isatin microarray experiments and for *cysP* for the 7-hydroxyindole microarray experiment. The results showed comparable changes in expression for the isatin arrays for *lsrA* (−37-fold in microarrays versus −72-fold with RT-PCR), for *lsrB* (−64-fold in microarrays versus −110-fold with RT-PCR), and for *lsrC*

(−18-fold in microarrays versus −41-fold with RT-PCR) as well as for *cysP* for the 7-hydroxyindole arrays (−11.8 in microarrays versus −17.3 with RT-PCR).

DISCUSSION

EHEC serotype O157:H7 is a human pathogen responsible for outbreaks of hemorrhagic colitis, causing bloody diarrhea that can lead to hemolytic-uremic syndrome, which affects mostly children around the world (7). However, to date, no effective therapy has been found (7, 68). Antibiotics, antimotility agents, narcotics, and nonsteroidal anti-inflammatory drugs are not usually provided, as they increase the risk of developing hemolytic-uremic syndrome, a major cause of acute renal failure in children (68). The LEE operon genes in a pathogenicity island are required for forming the attaching and effacing lesion to the host epithelial cells (45), and quorum-sensing signals (AI-2 and an unidentified AI-3) are involved in the quorum-sensing regulation of the LEE genes (60, 61). Bacterial biofilms are ubiquitous, and they have been extensively investigated under a variety of conditions. While there is increasing interest in bacterial biofilm formation in the gastrointestinal (GI) tract (30, 40), the genetic basis of EHEC biofilm formation is not well studied, whereas there are four single-time-point microarray studies of *E. coli* K-12 biofilm formation (5, 32, 51, 59) and one temporal study (11).

In this study, we found that EHEC serotype EDL933 forms robust biofilms under static conditions and a continuous-flow system. Surprisingly, biofilm cells formed on glass wool significantly repressed (3- to 11-fold) 20 pathogenic genes from the LEE island, compared to planktonic cells, which indicates that at 7 h, the virulence genes are not utilized yet. However, it is possible that the biofilm on glass wool lacks cues present for a biofilm on epithelial cells and that these cues may be necessary for induction of the virulence genes. It has been reported that the EPEC *espA* mutant formed more biofilms than wild-type EPEC (44). In our microarray data, *espA* was highly repressed (11-fold), along with repression of all the LEE operon genes, in the 7-h biofilm cells (see Table S1 in the supplemental material); however, EHEC biofilm formation in the GI tract may be different due to the presence of many signals from other GI bacteria and the host epithelial cells, unlike in the axenic glass wool culture used here. For example, we have determined that indole produced by *E. coli* K-12 and other commensal bacteria in the intestine affects EHEC chemotaxis and attachment (unpublished data), so indole is important for pathogenesis with EHEC. In addition, *yceK*, a predicted lipoprotein-encoding gene, is down-regulated eightfold in 7-h *E. coli* JM109 biofilms formed on glass wool (51) but was up-regulated eightfold in the EHEC biofilm; hence, this gene may play a different role in pathogenic *E. coli* or this may be an artifact of only a single time point used here. Also, colanic acid biosynthesis genes (*wcaABCDEFGHIJKL* and *rcsA*) are down-regulated in young (7-h) EHEC biofilm cells, as seen previously with asymptomatic bacteriuria *E. coli* (*galEKTU*) (23) and with nonpathogenic *E. coli* (*wcaJ*) (32). The fimbria-like gene *ycbQ* is down-regulated in *E. coli* K-12 BW25113 15-h biofilm cells (11) and was also repressed 14-fold in the EHEC biofilm. Also, *agaY*, a tagatose biphosphate aldolase gene, was induced fivefold in our data, which agrees well with earlier studies (11). Furthermore, nitrate reductase genes were significantly changed in this study (*narIGHK* are induced in biofilm cells, and *narUZYYW* are repressed with isatin), and *narVW* were induced in biofilm cells of *E. coli* K-12 PHL628 (32); hence, our data indicate that nitrate metabolism may play a role in the *E. coli* biofilm formation during the transition from aerobiosis to anaerobiosis (32).

For compounds to be called cell-to-cell signals, they must satisfy four criteria (72): (i) the putative signal must be produced during a specific stage (indole is produced primarily in the stationary phase (71), (ii) the putative signal must accumulate extracellularly and be recognized by a specific receptor (indole is a known extracellular signal [28, 53, 71] that is exported by AcrEF [34] and is imported by Mtr [77]), (iii) the putative signal must accumulate and generate a concerted response (indole has been shown to delay cell division [9]), and (iv) the putative signal must elicit a response that extends beyond the physiological changes required to metabolize or detoxify the signal (indole has been shown to control biofilms [36a] and cell division [9], which are not related to indole metabolism). Therefore, indole is a cell-to-cell signal molecule.

In this study, we demonstrate that hydroxylated indoles may be used to increase or decrease biofilm formation of pathogenic EHEC and that hydroxyindoles and isatin are interspecies biofilm signals. These results are important in that they indicate that the signal indole may undergo interference via oxygenase attack (by cells which do not synthesize it), with the result that the altered molecule influences the same phenotype (biofilm formation) in a different manner due to the presence of an unrelated strain. For example, unoxidized indole inhibits biofilm formation in EHEC while oxidized indole (isatin) stimulates it (Fig. 1). Therefore, this is another example where cells can detect the presence of other bacteria by the way their signals are manipulated (75). Furthermore, since hydroxyindoles are signals, this gives credence to our idea that some bacterial oxygenases may have evolved to regulate the concentrations of the interspecies signal indole by forming hydroxyindoles (36a). For example, wild-type toluene *o*-monooxygenase of *Burkholderia cepacia* G4 (56) hydroxylates indole to form primarily 7-hydroxyindole in *E. coli* (unpublished data), so 7-hydroxyindole is available for signaling. We are currently studying the mechanism by which indole and 7-hydroxyindole affect biofilm formation of *P. aeruginosa* PAO1 and have found that indole and 7-hydroxyindole (1,000 μM) do not cause toxicity or induce a stress response (unpublished data).

Previously, we found that cysteine biosynthetic genes (*cysPUWA*) were induced in biofilm cells at 7 and 15 h and in young biofilm cells at 4 h (11) and that a plant extract biofilm inhibitor, ursolic acid, repressed *cysDJK* (54). Also, deletion of *cysE* (65) or *cysB* (54) enhances biofilm formation in *E. coli*. Here, cysteine biosynthetic genes (*cysPD*) in biofilm cells were induced compared to those in planktonic cells, while 7-hydroxyindole most significantly repressed cysteine biosynthetic genes (*cysPJUIDA*) and isatin repressed cysteine desulferase genes (*sufABCDSE*) that convert cysteine into alanine and sulfane-sulfur (38) (see Table S1 in the supplemental material). It appears that isatin and 7-hydroxyindole both work through sulfur metabolism but do so in an opposite manner. Therefore, these results confirm that sulfur metabolism plays an important role in *E. coli* biofilm formation. It also appears

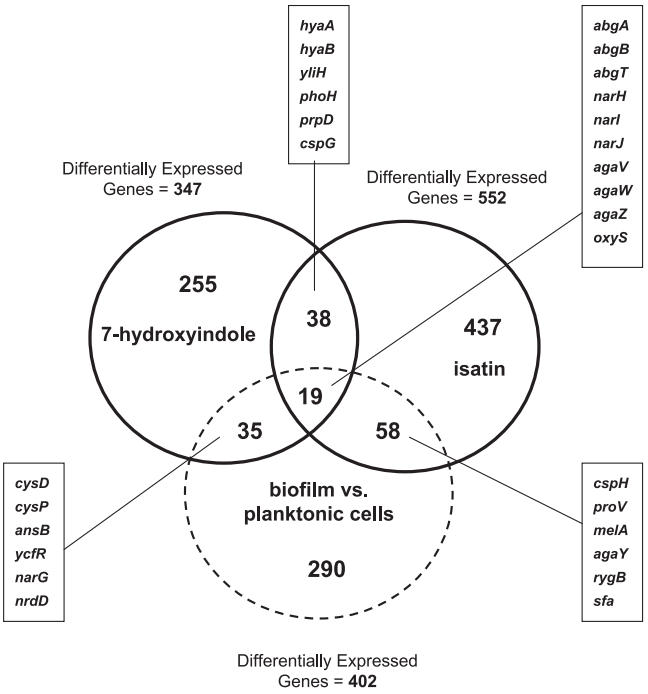

FIG. 5. Common differentially expressed genes between isatin (250 μM), 7-hydroxyindole (1,000 μM), and biofilm cells grown in LB medium at 30°C at 250 rpm for 7 h.

that 7-hydroxyindole and ursolic acid share a common mechanism of biofilm inhibition through sulfur metabolism. Unlike indole, 7-hydroxyindole does not work through SdiA in EHEC (no change of *sdiA* expression) and does not alter *sdiA* transcription in K-12, while indole inhibits *E. coli* K-12 biofilm formation through SdiA (36a).

In our temporal *E. coli* K-12 biofilm study, we found that motility and flagellar genes were induced in *E. coli* K-12 biofilm cells at 7 h and in planktonic cells or young biofilm cells at 4 h (11). In the current study, addition of isatin significantly induced 22 flagellar genes (*flgABCDEFGHIJK* and *fliAEF GILMNOPQ*) and repressed the AI-2 importers *lsrABCDF GKR* (see Table S1 in the supplemental material). In an analogous fashion, AI-2 induced the same flagellar genes (*flgAB CDEFGHIJKLMN* and *fliACDFHIKLMNOPQ*) in *E. coli* K-12 (52), and addition of AI-2 enhanced *E. coli* K-12 biofilm (20). Hence, isatin mimics AI-2 for stimulating biofilm formation. AI-2 concentrations were not altered by isatin (data not shown). Therefore, EHEC biofilm stimulation by isatin is not directly caused by AI-2 accumulation but is probably caused by the increased motility as a result of flagellar synthesis (74), the 20-fold reduction in indole concentration as a result of repression of *tnaA* (11, 12, 36a, 80), the changes in AI-2 transport, and the repression of sulfur metabolism (54, 65).

We determined the common differentially expressed genes between cells exposed to isatin and 7-hydroxyindole and for biofilm versus planktonic cells (Fig. 5). Totals of 347 and 552 genes were differentially expressed in the presence of 7-hydroxyindole and isatin, respectively, and for biofilm versus planktonic cells, the number of genes was 402. Of these, 19 genes were differentially expressed under all three conditions: *abgABT*, involved in *p*-aminobenzyl-glutamate utilization (31), *agaVWZ*, part of the *N*-acetylgalactosamine PTS system (8), and *narIJH*, associated with nitrate reductase (13), were all repressed in the presence of isatin and 7-hydroxyindole, whereas they were up-regulated in biofilm cells. Fifty-seven genes were common between isatin and 7-hydroxyindole cells, and the most prominent was the *hyaABCDE* operon, associated with hydrogenase (42), which was highly repressed in isatin biofilm cells. The hydrogenase genes *hyaABDEF*, as well as other hydrogenase genes (*hybAC* and *hycABF*), were significantly repressed in biofilm cells of *E. coli* K-12 MG1655 (59). The hydrogenases are probably used to regulate pH by removing the acid formate by converting it to CO_2 and H_2 (46), and hydrogenase 1 (*hya* operon) serves only to remove hydrogen (17), so if isatin represses these genes, then perhaps this is a result of internal pH changes induced by isatin. Furthermore, *yliH* was also repressed 9.8-fold by isatin, and since YliH represses biofilm formation (12), it is consistent that isatin repressed this gene while increasing biofilm formation. *oxyS* RNA is involved in detoxifying oxidative damage (21); this locus was induced 4.6-fold by isatin, and this indicates that isatin may also cause oxidative stress, as has been seen with K-12 biofilms previously (51). Seventy-seven genes were common between isatin-treated cells and biofilm cells, and 54 genes were common between 7-hydroxyindole-treated cells and biofilm cells.

In this study, we verified the hypothesis that hydroxyindoles may be signals, based on our recognition of the large extracellular indole concentrations and the prevalence of relatively nonspecific oxygenases that can hydroxylate indole, such as monooxygenases and dioxygenases in *Pseudomonas*, *Ralstonia*, and *Burkholderia* species (15, 16, 56). It was found that indole, 5-hydroxyindole, and 7-hydroxyindole are potent inhibitors of EHEC biofilm formation (which suggests their use as potential therapeutics), whereas isatin stimulates biofilm formation. Along with brominated furanones (52) and ursolic acid (54), 7-hydroxyindole becomes one of the few known nontoxic biofilm inhibitors.

ACKNOWLEDGMENTS

This research was supported by the NIH (EB003872-01A1) and ARO (W911NF-06-1-0408).

We thank Tim McDermott for the *P. aeruginosa* PAO1 strain.

REFERENCES

1. **Anyanful, A., J. M. Dolan-Livengood, T. Lewis, S. Sheth, M. N. Dezalia, M. A. Sherman, L. V. Kalman, G. M. Benian, and D. Kalman.** 2005. Paralysis and killing of *Caenorhabditis elegans* by enteropathogenic *Escherichia coli* requires the bacterial tryptophanase gene. Mol. Microbiol. **57:**988–1007.
2. **Baba, T., T. Ara, M. Hasegawa, Y. Takai, Y. Okumura, M. Baba, K. A. Datsenko, M. Tomita, B. L. Wanner, and H. Mori.** 2006. Construction of *Escherichia coli* K-12 in-frame, single-gene knockout mutants: the Keio collection. Mol. Syst. Biol. **2:**2006.0008.
3. **Baca-DeLancey, R. R., M. M. South, X. Ding, and P. N. Rather.** 1999. *Escherichia coli* genes regulated by cell-to-cell signaling. Proc. Natl. Acad. Sci. USA **96:**4610–4614.
4. **Barrett, T., T. O. Suzek, D. B. Troup, S. E. Wilhite, W. C. Ngau, P. Ledoux, D. Rudnev, A. E. Lash, W. Fujibuchi, and R. Edgar.** 2005. NCBI GEO: mining millions of expression profiles—database and tools. Nucleic Acids Res. **33:**D562–D566.
5. **Beloin, C., J. Valle, P. Latour-Lambert, P. Faure, M. Kzreminski, D. Balestrino, J. A. Haagensen, S. Molin, G. Prensier, B. Arbeille, and J. M. Ghigo.** 2004. Global impact of mature biofilm lifestyle on *Escherichia coli* K-12 gene expression. Mol. Microbiol. **51:**659–674.
6. **Boos, W., U. Ehmann, H. Forkl, W. Klein, M. Rimmele, and P. Postma.** 1990. Trehalose transport and metabolism in *Escherichia coli*. J. Bacteriol. **172:** 3450–3461.

7. **Boyce, T. G., D. L. Swerdlow, and P. M. Griffin.** 1995. *Escherichia coli* O157:H7 and the hemolytic-uremic syndrome. N. Engl. J. Med. **333:**364–368.
8. **Brinkkötter, A., H. Klöβ, C. Alpert, and J. W. Lengeler.** 2000. Pathways for the utilization of N-acetyl-galactosamine and galactosamine in *Escherichia coli*. Mol. Microbiol. **37:**125–135.
9. **Chant, E. L., and D. K. Summers.** 2007. Indole signalling contributes to the stable maintenance of *Escherichia coli* multicopy plasmids. Mol. Microbiol. **63:**35–43.
10. **Davies, D. G., M. R. Parsek, J. P. Pearson, B. H. Iglewski, J. W. Costerton, and E. P. Greenberg.** 1998. The involvement of cell-to-cell signals in the development of a bacterial biofilm. Science **280:**295–298.
11. **Domka, J., J. Lee, T. Bansal, and T. K. Wood.** 2007. Temporal gene-expression in *Escherichia coli* K-12 biofilms. Environ. Microbiol. **9:**332–346.
12. **Domka, J., J. Lee, and T. K. Wood.** 2006. YliH (BssR) and YceP (BssS) regulate *Escherichia coli* K-12 biofilm formation by influencing cell signaling. Appl. Environ. Microbiol. **72:**2449–2459.
13. **Dubourdieu, M., and J. A. DeMoss.** 1992. The *narJ* gene product is required for biogenesis of respiratory nitrate reductase in *Escherichia coli*. J. Bacteriol. **174:**867–872.
14. **Edgar, R., M. Domrachev, and A. E. Lash.** 2002. Gene Expression Omnibus: NCBI gene expression and hybridization array data repository. Nucleic Acids Res. **30:**207–210.
15. **Ensley, B. D., B. J. Ratzkin, T. D. Osslund, M. J. Simon, L. P. Wackett, and D. T. Gibson.** 1983. Expression of naphthalene oxidation genes in *Escherichia coli* results in the biosynthesis of indigo. Science **222:**167–169.
16. **Fishman, A., Y. Tao, L. Rui, and T. K. Wood.** 2005. Controlling the regiospecific oxidation of aromatics via active site engineering of toluene *para*-monooxygenase of *Ralstonia pickettii* PKO1. J. Biol. Chem. **280:**506–514.
17. **Forzi, L., and R. G. Sawers.** 2007. Maturation of [NiFe]-hydrogenases in *Escherichia coli*. Biometals **20:**565–575.
18. **Frenzen, P. D., A. Drake, and F. J. Angulo.** 2005. Economic cost of illness due to *Escherichia coli* O157 infections in the United States. J. Food Prot. **68:**2623–2630.
19. **García-Lara, J., L. H. Shang, and L. I. Rothfield.** 1996. An extracellular factor regulates expression of *sdiA*, a transcriptional activator of cell division genes in *Escherichia coli*. J. Bacteriol. **178:**2742–2748.
20. **González Barrios, A. F., R. Zuo, Y. Hashimoto, L. Yang, W. E. Bentley, and T. K. Wood.** 2006. Autoinducer 2 controls biofilm formation in *Escherichia coli* through a novel motility quorum-sensing regulator (MqsR, B3022). J. Bacteriol. **188:**305–316.
21. **Gottesman, S.** 2004. The small RNA regulators of *Escherichia coli*: roles and mechanisms. Annu. Rev. Microbiol. **58:**303–328.
22. **Hammer, B. K., and B. L. Bassler.** 2003. Quorum sensing controls biofilm formation in *Vibrio cholerae*. Mol. Microbiol. **50:**101–104.
23. **Hancock, V., and P. Klemm.** 2007. Global gene expression profiling of asymptomatic bacteriuria *Escherichia coli* during biofilm growth in human urine. Infect. Immun. **75:**966–976.
24. **Hansen, M. C., R. J. Palmer, Jr., C. Udsen, D. C. White, and S. Molin.** 2001. Assessment of GFP fluorescence in cells of *Streptococcus gordonii* under conditions of low pH and low oxygen concentration. Microbiology **147:**1383–1391.
25. **Hentzer, M., H. Wu, J. B. Andersen, K. Riedel, T. B. Rasmussen, N. Bagge, N. Kumar, M. A. Schembri, Z. Song, P. Kristoffersen, M. Manefield, J. W. Costerton, S. Molin, L. Eberl, P. Steinberg, S. Kjelleberg, N. Hoiby, and M. Givskov.** 2003. Attenuation of *Pseudomonas aeruginosa* virulence by quorum sensing inhibitors. EMBO J. **22:**3803–3815.
26. **Herzberg, M., I. K. Kaye, W. Peti, and T. K. Wood.** 2006. YdgG (TqsA) controls biofilm formation in *Escherichia coli* K-12 through autoinducer 2 transport. J. Bacteriol. **188:**587–598.
27. **Heydorn, A., A. T. Nielsen, M. Hentzer, C. Sternberg, M. Givskov, B. K. Ersboll, and S. Molin.** 2000. Quantification of biofilm structures by the novel computer program COMSTAT. Microbiology **146:**2395–2407.
28. **Hirakawa, H., Y. Inazumi, T. Masaki, T. Hirata, and A. Yamaguchi.** 2005. Indole induces the expression of multidrug exporter genes in *Escherichia coli*. Mol. Microbiol. **55:**1113–1126.
29. **Hoessel, R., S. Leclerc, J. A. Endicott, M. E. Nobel, A. Lawrie, P. Tunnah, M. Leost, E. Damiens, D. Marie, D. Marko, E. Niederberger, W. Tang, G. Eisenbrand, and L. Meijer.** 1999. Indirubin, the active constituent of a Chinese antileukaemia medicine, inhibits cyclin-dependent kinases. Nat. Cell Biol. **1:**60–67.
30. **Huijsdens, X. W., R. K. Linskens, M. Mak, S. G. Meuwissen, C. M. Vandenbroucke-Grauls, and P. H. Savelkoul.** 2002. Quantification of bacteria adherent to gastrointestinal mucosa by real-time PCR. J. Clin. Microbiol. **40:**4423–4427.
31. **Hussein, M. J., J. M. Green, and B. P. Nichols.** 1998. Characterization of mutations that allow *p*-aminobenzoyl-glutamate utilization by *Escherichia coli*. J. Bacteriol. **180:**6260–6268.
32. **Junker, L. M., J. E. Peters, and A. G. Hay.** 2006. Global analysis of candidate genes important for fitness in a competitive biofilm using DNA-array-based transposon mapping. Microbiology **152:**2233–2245.
33. **Kaper, J. B., and V. Sperandio.** 2005. Bacterial cell-to-cell signaling in the gastrointestinal tract. Infect. Immun. **73:**3197–3209.
34. **Kawamura-Sato, K., K. Shibayama, T. Horii, Y. Iimuma, Y. Arakawa, and M. Ohta.** 1999. Role of multiple efflux pumps in *Escherichia coli* in indole expulsion. FEMS Microbiol. Lett. **179:**345–352.
35. **Kitagawa, M., T. Ara, M. Arifuzzaman, T. Ioka-Nakamichi, E. Inamoto, H. Toyonaga, and H. Mori.** 2005. Complete set of ORF clones of *Escherichia coli* ASKA library (a complete set of *E. coli* K-12 ORF archive): unique resources for biological research. DNA Res. **12:**291–299.
36. **Labbate, M., S. Y. Queck, K. S. Koh, S. A. Rice, M. Givskov, and S. Kjelleberg.** 2004. Quorum sensing-controlled biofilm development in *Serratia liquefaciens* MG1. J. Bacteriol. **186:**692–698.

36a. **Lee, J., A. Jayaraman, and T. K. Wood.** 2007. Indole is an inter-species biofilm signal mediated by SdiA. BMC Microbiol. **7:**42.

37. **Leveau, J. H., and S. E. Lindow.** 2005. Utilization of the plant hormone indole-3-acetic acid for growth by *Pseudomonas putida* strain 1290. Appl. Environ. Microbiol. **71:**2365–2371.
38. **Loiseau, L., S. Ollagnier-de-Choudens, L. Nachin, M. Fontecave, and F. Barras.** 2003. Biogenesis of Fe-S cluster by the bacterial Suf system: SufS and SufE form a new type of cysteine desulfurase. J. Biol. Chem. **278:**38352–38359.
39. **Lombardía, E., A. J. Rovetto, A. L. Arabolaza, and R. R. Grau.** 2006. A LuxS-dependent cell-to-cell language regulates social behavior and development in *Bacillus subtilis*. J. Bacteriol. **188:**4442–4452.
40. **Macfarlane, S., and G. T. Macfarlane.** 2006. Composition and metabolic activities of bacterial biofilms colonizing food residues in the human gut. Appl. Environ. Microbiol. **72:**6204–6211.
41. **McNab, R., S. K. Ford, A. El-Sabaeny, B. Barbieri, G. S. Cook, and R. J. Lamont.** 2003. LuxS-based signaling in *Streptococcus gordonii:* autoinducer 2 controls carbohydrate metabolism and biofilm formation with *Porphyromonas gingivalis*. J. Bacteriol. **185:**274–284.
42. **Menon, N. K., J. Robbins, J. C. Wendt, K. T. Shanmugam, and A. E. Przybyla.** 1991. Mutational analysis and characterization of the *Escherichia coli hya* operon, which encodes [NiFe] hydrogenase 1. J. Bacteriol. **173:**4851–4861.
43. **Michael, B., J. N. Smith, S. Swift, F. Heffron, and B. M. Ahmer.** 2001. SdiA of *Salmonella enterica* is a LuxR homolog that detects mixed microbial communities. J. Bacteriol. **183:**5733–5742.
44. **Moreira, C. G., K. Palmer, M. Whiteley, M. P. Sircili, L. R. Trabulsi, A. F. Castro, and V. Sperandio.** 2006. Bundle-forming pili and EspA are involved in biofilm formation by enteropathogenic *Escherichia coli*. J. Bacteriol. **188:**3952–3961.
45. **Nataro, J. P., and J. B. Kaper.** 1998. Diarrheagenic *Escherichia coli*. Clin. Microbiol. Rev. **11:**142–201.
46. **Neidhardt, F. C. (ed.).** 1996. *Escherichia coli* and *Salmonella*: cellular and molecular biology, 2nd ed., vol. 1. ASM Press, Washington, DC.
47. **Newton, W. A., and E. E. Snell.** 1965. Formation and interrelationships of tryptophanase and tryptophan synthetases in *Escherichia coli*. J. Bacteriol. **89:**355–364.
48. **Perna, N. T., G. F. Mayhew, G. Posfai, S. Elliott, M. S. Donnenberg, J. B. Kaper, and F. R. Blattner.** 1998. Molecular evolution of a pathogenicity island from enterohemorrhagic *Escherichia coli* O157:H7. Infect. Immun. **66:**3810–3817.
49. **Pratt, L. A., and R. Kolter.** 1998. Genetic analysis of *Escherichia coli* biofilm formation: roles of flagella, motility, chemotaxis and type I pili. Mol. Microbiol. **30:**285–293.
50. **Prigent-Combaret, C., O. Vidal, C. Dorel, and P. Lejeune.** 1999. Abiotic surface sensing and biofilm-dependent regulation of gene expression in *Escherichia coli*. J. Bacteriol. **181:**5993–6002.
51. **Ren, D., L. A. Bedzyk, S. M. Thomas, R. W. Ye, and T. K. Wood.** 2004. Gene expression in *Escherichia coli* biofilms. Appl. Microbiol. Biotechnol. **64:**515–524.
52. **Ren, D., L. A. Bedzyk, R. W. Ye, S. M. Thomas, and T. K. Wood.** 2004. Differential gene expression shows natural brominated furanones interfere with the autoinducer-2 bacterial signaling system of *Escherichia coli*. Biotechnol. Bioeng. **88:**630–642.
53. **Ren, D., L. A. Bedzyk, R. W. Ye, S. M. Thomas, and T. K. Wood.** 2004. Stationary-phase quorum-sensing signals affect autoinducer-2 and gene expression in *Escherichia coli*. Appl. Environ. Microbiol. **70:**2038–2043.
54. **Ren, D., R. Zuo, A. F. González Barrios, L. A. Bedzyk, G. R. Eldridge, M. E. Pasmore, and T. K. Wood.** 2005. Differential gene expression for investigation of *Escherichia coli* biofilm inhibition by plant extract ursolic acid. Appl. Environ. Microbiol. **71:**4022–4034.
55. **Rickard, A. H., R. J. Palmer, Jr., D. S. Blehert, S. R. Campagna, M. F. Semmelhack, P. G. Egland, B. L. Bassler, and P. E. Kolenbrander.** 2006. Autoinducer 2: a concentration-dependent signal for mutualistic bacterial biofilm growth. Mol. Microbiol. **60:**1446–1456.
56. **Rui, L., K. F. Reardon, and T. K. Wood.** 2005. Protein engineering of toluene *ortho*-monooxygenase of *Burkholderia cepacia* G4 for regiospecific hydroxylation of indole to form various indigoid compounds. Appl. Microbiol. Biotechnol. **66:**422–429.
57. **Ryu, J. H., and L. R. Beuchat.** 2005. Biofilm formation by *Escherichia coli* O157:H7 on stainless steel: effect of exopolysaccharide and curli production on its resistance to chlorine. Appl. Environ. Microbiol. **71:**247–254.

58. **Sambrook, J., E. F. Fritsch, and T. Maniatis.** 1989. Molecular cloning: a laboratory manual, 2nd ed. Cold Spring Harbor Laboratory Press, Cold Spring Harbor, NY.
59. **Schembri, M. A., K. Kjaergaard, and P. Klemm.** 2003. Global gene expression in *Escherichia coli* biofilms. Mol. Microbiol. **48:**253–267.
60. **Sperandio, V., J. L. Mellies, W. Nguyen, S. Shin, and J. B. Kaper.** 1999. Quorum sensing controls expression of the type III secretion gene transcription and protein secretion in enterohemorrhagic and enteropathogenic *Escherichia coli*. Proc. Natl. Acad. Sci. USA **96:**15196–15201.
61. **Sperandio, V., A. G. Torres, B. Jarvis, J. P. Nataro, and J. B. Kaper.** 2003. Bacteria-host communication: the language of hormones. Proc. Natl. Acad. Sci. USA **100:**8951–8956.
62. **Sperandio, V., A. G. Torres, and J. B. Kaper.** 2002. Quorum sensing *Escherichia coli* regulators B and C (QseBC): a novel two-component regulatory system involved in the regulation of flagella and motility by quorum sensing in *E. coli*. Mol. Microbiol. **43:**809–821.
63. **Stover, C. K., X. Q. Pham, A. L. Erwin, S. D. Mizoguchi, P. Warrener, M. J. Hickey, F. S. Brinkman, W. O. Hufnagle, D. J. Kowalik, M. Lagrou, R. L. Garber, L. Goltry, E. Tolentino, S. Westbrock-Wadman, Y. Yuan, L. L. Brody, S. N. Coulter, K. R. Folger, A. Kas, K. Larbig, R. Lim, K. Smith, D. Spencer, G. K. Wong, Z. Wu, I. T. Paulsen, J. Reizer, M. H. Saier, R. E. Hancock, S. Lory, and M. V. Olson.** 2000. Complete genome sequence of *Pseudomonas aeruginosa* PAO1, an opportunistic pathogen. Nature **406:**959–964.
64. **Strockbine, N. A., L. R. Marques, J. W. Newland, H. W. Smith, R. K. Holmes, and A. D. O'Brien.** 1986. Two toxin-converting phages from *Escherichia coli* O157:H7 strain 933 encode antigenically distinct toxins with similar biologic activities. Infect. Immun. **53:**135–140.
65. **Sturgill, G., C. M. Toutain, J. Komperda, G. A. O'Toole, and P. N. Rather.** 2004. Role of CysE in production of an extracellular signaling molecule in *Providencia stuartii* and *Escherichia coli*: loss of CysE enhances biofilm formation in *Escherichia coli*. J. Bacteriol. **186:**7610–7617.
66. **Surette, M. G., and B. L. Bassler.** 1998. Quorum sensing in *Escherichia coli* and *Salmonella typhimurium*. Proc. Natl. Acad. Sci. USA **95:**7046–7050.
67. **Tao, Y., A. Fishman, W. E. Bentley, and T. K. Wood.** 2004. Altering toluene 4-monooxygenase by active-site engineering for the synthesis of 3-methoxycatechol, methoxyhydroquinone, and methylhydroquinone. J. Bacteriol. **186:**4705–4713.
68. **Tarr, P. I., C. A. Gordon, and W. L. Chandler.** 2005. Shiga-toxin-producing *Escherichia coli* and haemolytic uraemic syndrome. Lancet **365:**1073–1086.
69. **Uhlich, G. A., P. H. Cooke, and E. B. Solomon.** 2006. Analyses of the red-dry-rough phenotype of an *Escherichia coli* O157:H7 strain and its role in biofilm formation and resistance to antibacterial agents. Appl. Environ. Microbiol. **72:**2564–2572.
70. **Walters, M., and V. Sperandio.** 2006. Autoinducer 3 and epinephrine signaling in the kinetics of locus of enterocyte effacement gene expression in enterohemorrhagic *Escherichia coli*. Infect. Immun. **74:**5445–5455.
71. **Wang, D., X. Ding, and P. N. Rather.** 2001. Indole can act as an extracellular signal in *Escherichia coli*. J. Bacteriol. **183:**4210–4216.
72. **Winzer, K., K. R. Hardie, and P. Williams.** 2002. Bacterial cell-to-cell communication: sorry, can't talk now—gone to lunch! Curr. Opin. Microbiol. **5:**216–222.
73. **Wong, C. S., S. Jelacic, R. L. Habeeb, S. L. Watkins, and P. I. Tarr.** 2000. The risk of the hemolytic-uremic syndrome after antibiotic treatment of *Escherichia coli* O157:H7 infections. N. Engl. J. Med. **342:**1930–1936.
74. **Wood, T. K., A. F. González Barrios, M. Herzberg, and J. Lee.** 2006. Motility influences biofilm architecture in *Escherichia coli*. Appl. Microbiol. Biotechnol. **72:**361–367.
75. **Xavier, K. B., and B. L. Bassler.** 2005. Interference with AI-2-mediated bacterial cell-cell communication. Nature **437:**750–753.
76. **Yang, F., L. H. Wang, J. Wang, Y. H. Dong, J. Y. Hu, and L. H. Zhang.** 2005. Quorum quenching enzyme activity is widely conserved in the sera of mammalian species. FEBS Lett. **579:**3713–3717.
77. **Yanofsky, C., V. Horn, and P. Gollnick.** 1991. Physiological studies of tryptophan transport and tryptophanase operon induction in *Escherichia coli*. J. Bacteriol. **173:**6009–6017.
78. **Yao, Y., M. A. Martinez-Yamout, T. J. Dickerson, A. P. Brogan, P. E. Wright, and H. J. Dyson.** 2006. Structure of the *Escherichia coli* quorum sensing protein SdiA: activation of the folding switch by acyl homoserine lactones. J. Mol. Biol. **355:**262–273.
79. **Zhang, L. H., and Y. H. Dong.** 2004. Quorum sensing and signal interference: diverse implications. Mol. Microbiol. **53:**1563–1571.
80. **Zhang, X. S., R. Garcia-Contreras, and T. K. Wood.** 2007. YcfR (BhsA) influences *Escherichia coli* biofilm formation through stress response and surface hydrophobicity. J. Bacteriol. **189:**3051–3062.